Annals of Glaciology 29 1999

Chemical characterisation of a volcanic event (about AD 1500) at Styx Glacier plateau, northern Victoria Land, Antarctica

R. Udisti,[1*] C. Barbante,[2,3] E. Castellano,[4] S. Vermigli,[4] R. Traversi,[4]
G. Capodaglio,[2,3] G. Piccardi[4]

[1]*Department of Chemistry, University of Calabria, I-87030 Arcavacata di Rende (Cosenza), Italy*
[2]*Department of Environmental Science, University of Venice, Dorsoduro 2137, I-30123 Venice, Italy*
[3]*Centro di Studio sulla Chimica e le Tecnologie per l'Ambiente — CNR, I-30123 Venice, Italy*
[4]*Department of Public Health and Environmental Analytical Chemistry, University of Florence, Via G. Capponi 9, I-50121 Florence, Italy*

ABSTRACT. A dark layer (~1 cm thick, 93.41 m deep) was identified in an ice core (116 m deep, covering the period ~1350–1995) drilled at Styx Glacier plateau, northern Victoria Land, Antarctica. The ice-core section was dated around AD 1500 ± 20 by a firn-densification model. A chemical characterisation was performed on ten subsamples (resolution 3 cm) located around the dark layer by ion chromatography. The concentration/depth profiles of anions (Cl^-, Br^-, NO_3^-, $H_2PO_4^-$, SO_4^{2-}), cations (Na^+, NH_4^+, K^+, Mg^{2+}, Ca^{2+}) and some organic anions (acetate, formate, propionate and methanesulphonate (MSA)) indicate very high concentration peaks for all the components. However, non-sea-salt sulphate ($nssSO_4^{2-}$) and F^- show the greatest increase with respect to background values (370 and 860 times, respectively). A crustal contribution is attributed to Ca^{2+} and MSA. The profiles of gas-phase emitted substances (HF, HBr, HNO_3 and carboxylic acid) suggest gas emission just before the volcanic eruption. Chloride depletion is evident in the dark layer with respect to Na^+/Cl^- sea-water ratio. At present, it is not possible to attribute an unambiguous source to the volcanic event, but several pieces of evidence lead us to believe that this may be a time-limited local event.

INTRODUCTION

The temporal distribution of environmental tracer substances can be determined by analyzing successive snow layers of ice cores sampled in the ice caps. Such a study constitutes an effective method to:

- identify the principal and secondary sources of atmospheric aerosols such as sea spray, marine biogenic, volcanic, crustal or anthropogenic inputs;
- understand the transport processes of environmentally relevant substances, with particular attention to sea/atmosphere/snow interface exchange;
- highlight particular events capable of putting into the atmosphere high quantities of well-defined compounds (e.g. volcanic eruptions, biomass-burning, nuclear experiments or accidents).

In particular, volcanic input is one of the main aerosol sources and the most important localised geochemical source. Volcanic eruptions can introduce into the atmosphere significant quantities of H_2SO_4, HCl, HF and HBr (10, 8, 0.4 and 0.08 × 10^{12} g a^{-1}, respectively; Brimblecombe, 1996), and, in the case of an explosive eruption, gas and particulate can be injected into the highest part of the troposphere or directly into the stratosphere, with high half-life times and global-scale diffusion (Hammer and others, 1980; Legrand and Delmas, 1987; Clausen and Hammer, 1988; Delmas and others, 1992; Aristarain and Delmas, 1998).

In areas characterised by low crustal and anthropogenic contributions, such as Antarctica, volcanic emissions can constitute a fundamental input to the atmospheric aerosol composition. The gas-phase substances and particulate content can play a relevant role in environmental and climate variations, by means of sunlight-scattering processes and formation and growth of cloud-condensation nuclei (Hammer and others, 1980; Handler, 1989; Rampino and Self, 1992; Zreda-Gostynska and others, 1997). Besides, the identification of historically known volcanic events in ice cores is the main technique for obtaining reference horizons for a reliable absolute dating of the sampled snow layers (Langway and others, 1988; Hammer, 1989; Delmas and others, 1992). Volcanic levels can be identified mainly by high and sudden increases of specific markers such as sulphate, fluoride, bromide, chloride (from the related acids), carboxylic acids, ash and total acidity, and of non-specific parameters, such as dielectric properties and electrical conductivity (Hammer and others 1980; Palais and others, 1990; Aristarain and Delmas, 1998).

In this paper we report the chemical characterisation by ion chromatographic (IC) analysis of a volcanic event recorded in an ice core drilled on Styx Glacier plateau (1750 m a.s.l.), northern Victoria Land, East Antarctica. The volcanic event was shown by a dark layer at 93.41 m depth and dated to about AD 1500.

* Present address: Analytical Chemistry Section, University of Florence, Via G. Capponi 9, 1-50127 Florence, Italy.

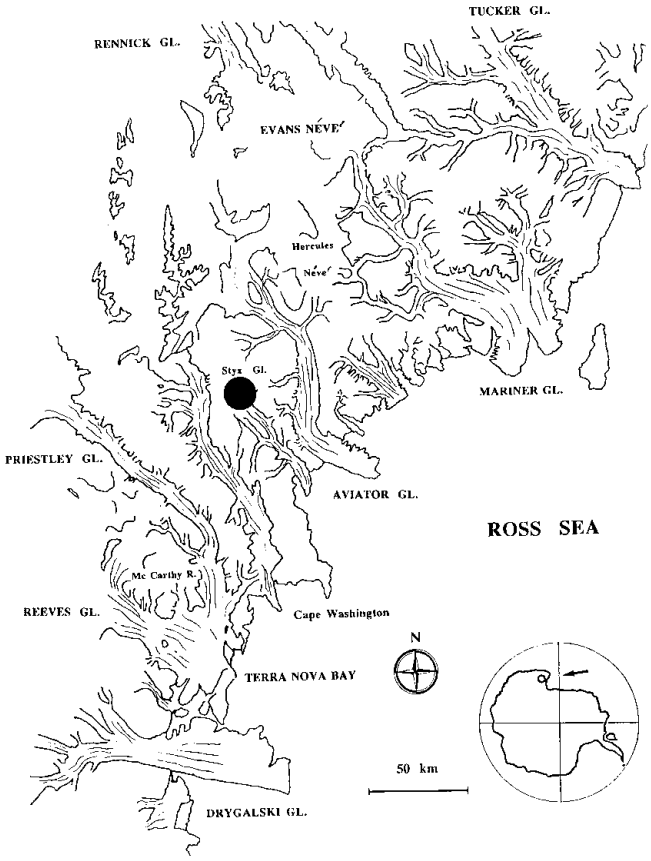

Fig. 1. Map of sampling station: Styx Glacier plateau, northern Victoria Land, Antarctica (163° 56′ E, 73° 52′ S; 1750 m a.s.l.).

EXPERIMENTAL

Sampling station

The ice-core sampling station, Styx Glacier plateau (163°56′ E, 73°52′ S; 1750 m a.s.l.), is shown in Figure 1. The Styx Glacier plateau is a 150 km^2 plateau, located between the Campbell Glacier and Tinker Glacier valleys, about 50 km from the coastline (Wood Bay) and at 1600–1800 m a.s.l. This area was chosen by satellite observations of snow morphology in the area of Terra Nova Bay (about 100 000 km^2 in northern Victoria Land), which were used to isolate stations where wind-redistribution effects (shown by blue ice, sastrugi or snowdrift areas) are as low as possible (Stenni and others, unpublished). In fact, several authors (e.g. Pettre and others, 1986; Goodwin, 1990) have pointed out the importance of katabatic winds for the net annual snow-accumulation rate. Transport (ablation, accumulation and redistribution) processes can change the snow-layer sequence, making the reconstruction of successive depositions impossible. The Styx Glacier plateau wind-field analysis indicated that the Campbell Glacier valley channels the katabatic winds coming from the west and northwest, so that only moderate snowdrifts (west–east oriented) are present.

At this station, snow and firn samples were collected in snow pits and shallow firn cores during several Italian Antarctic campaigns. The samples were analyzed to determine the chemical composition of snow and the mean snow-accumulation rate. These results are reported in Piccardi and others (1994a, b, 1996a, b) Udisti (1996) and Udisti and others (1998b) with the following conclusions:

(1) a well-defined seasonal signal for H_2O_2, non-sea-salt sulphate ($nssSO_4^{2-}$), methanesulphonate (MSA) and $\delta^{18}O$ is present, and therefore such compounds can be used as seasonal markers (high summer values). This evidence confirms an undisturbed snow-layer sequence;

(2) ice crusts showing summer snow melting are missing, due to the rather high elevation (about 1700 m a.s.l.);

(3) a fairly high mean annual accumulation rate of about 160 kg m^{-2} a^{-1} w.e. allows a good temporal resolution of the sampled snow layers.

For the above reasons, the Styx station was chosen as a site for medium-depth ice-coring in the 1995–96 Italian campaign.

Ice-core sampling

The Styx Glacier ice core (116 m deep) was drilled in November 1995 using a wire-driven corer ICE-DRILL 4 (FS INVENTOR AG, Switzerland). This drill collects 107 mm diameter ice cores with a maximum length of 950 mm per run, operating at a maximum depth of 150 m. The single ice-core sections obtained step by step were externally cleaned on site and closed in double-sealed polyethylene bags. The ice-core sections were weighed to determine their density; the values range from 0.38 g cm^{-3} (superficial layers) to 0.73–0.98 g cm^{-3} for layers deeper than 80 m. During the ice-core collection and handling, care was taken to minimise contamination (clean-room clothes, facial masks and polyethylene gloves).

Visual examination of an ice-core section showed a thin, dark layer (about 10 mm thick) located at 93.41 m. An interval of 300 mm around the dark layer was immediately subsampled and analyzed. This ice-core section was divided into ten subsamples with a resolution of 30 mm.

All decontamination (by mechanical removal of a 10 mm external layer with a hand scraper) and cutting operations were performed in a cold room under a class 100 laminar hood. Each sample manipulation was previously controlled by a similar operation performed on a synthetic ice core obtained from ultra-pure water to minimise the contamination. The operational blank shows contamination levels 1–2 orders of magnitude lower than the lowest measured concentrations ("background" level measured on the samples far away from the dark layer).

Ice-core approximate dating

At the time of writing, the subsampling of the remaining ice core is still in progress, so an accurate dating of the ice core is not yet available. An approximate dating was estimated using the firn-densification model of Herron and Langway (1980) to model the density data obtained from the weight and area measurements on all the ice-core sections (Ling, 1985). Figure 2a shows the experimental density/depth profile. These data have been fitted on the basis of the following equation proposed by Herron and Langway (1980):

$$\frac{\rho - \rho_0}{\rho_m - \rho_0} = 1 - e^{-x/L},$$

where ρ and x are the density and depth, respectively. ρ_0, ρ_m and L are the calculated parameters of the fitting: ρ_0 (0.41 g cm^{-3}) is the density of surface snow, ρ_m (0.87 g cm^{-3}) is the maximum density in the dry-snow zone and L (27) is a parameter characteristic of the sampling site. Considering a mean annual accumulation of 160 kg m^{-2} a^{-1} w.e. and taking into account the relationship between density, accumu-

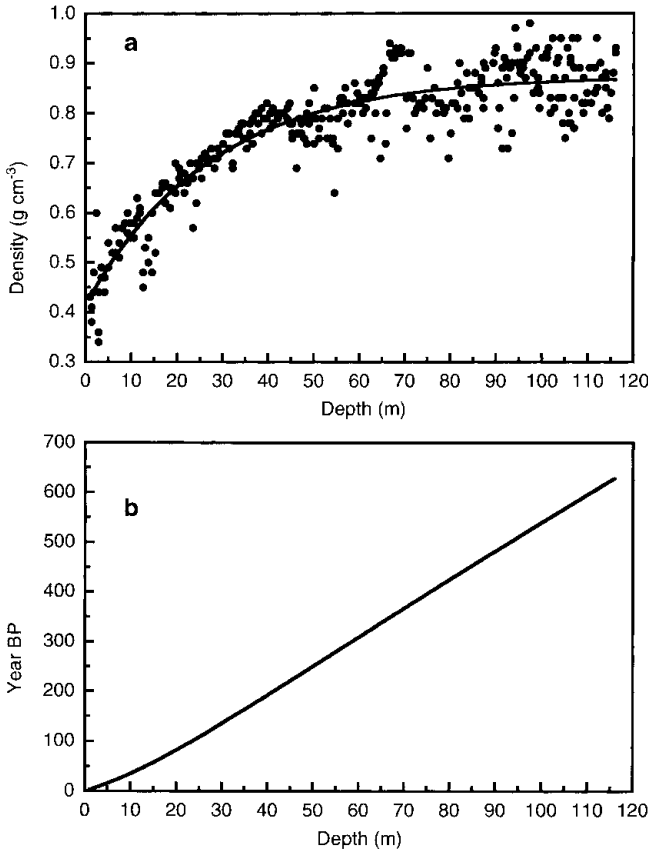

Fig. 2. Ice-core dating by the firn-densification model of Herron and Langway (1980) to model the density data (Ling, 1985). (a) Experimental density/depth profile. (b) Age/depth curve obtained considering a mean annual accumulation of 160 kg m^{-2} a^{-1} w.e. This curve has been used to extrapolate the age of the ice-core section in which the volcanic layer was found (93.41 m depth).

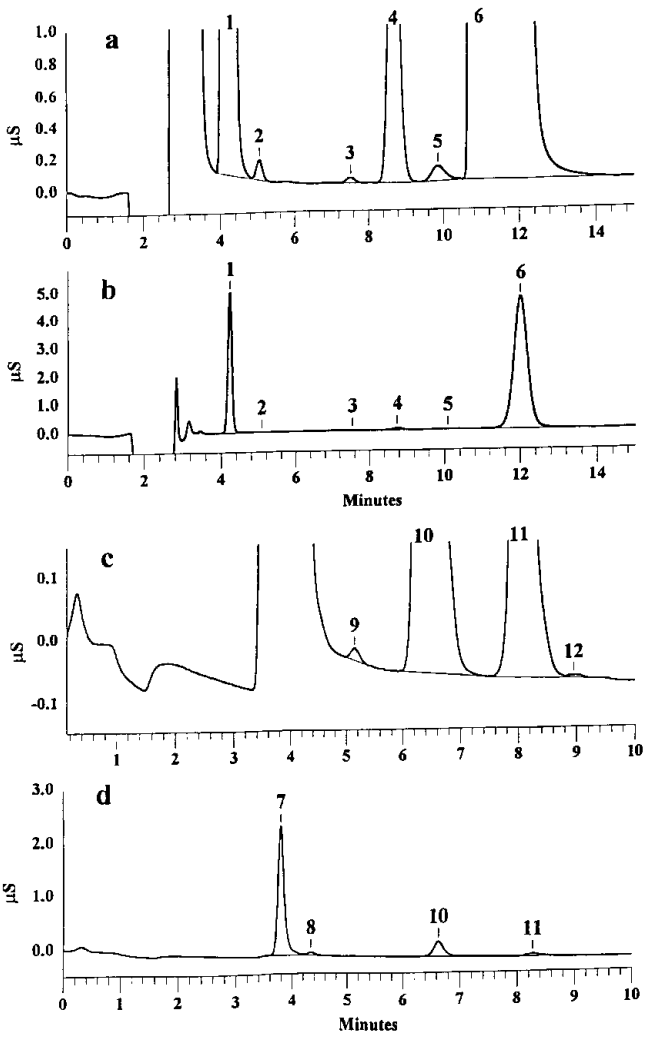

Fig. 3. Ion chromatograms for sample 7 (93.41 m depth) of inorganic anions without dilution (a) and at 1:40 dilution (b); and organic anions plus fluoride without dilution (c) and at 1:40 dilution (d). 1. Chloride, 2. Nitrite, 3. Bromide, 4. Nitrate, 5. Phosphate, 6. Sulphate, 7. Fluoride, 8. Acetate, 9. Propionate, 10. Formate, 11. MSA, 12. Pyruvate. Concentration values are given in Table 2.

lation rate and depth, it is possible to plot the age/depth curve as shown in Figure 2b. This curve has been used to extrapolate the age of the ice-core section in which the volcanic layer was found.

According to this model, the whole ice core covers approximately the period AD 1995–1350, so the oldest layers (depth 116 m) can be attributed to snow precipitation about 650 years ago. The age of the dark layer, located at 93.41 m depth, can be estimated at about 500 ± 20 years (around AD 1500).

Chemical analysis

The subsamples were melted in their closed containers, and IC measurements were performed immediately after melting to avoid gas-phase contaminant uptake (above all, ammonia and carboxylic acids; Udisti and others, 1991, 1994). At the IC injection time, the samples were filtered on a 0.45 μm teflon membrane, chosen as a conventional limit between the soluble and insoluble fractions. Therefore, the chemical analysis is related only to the soluble components (particle dimension <0.45 μm).

IC methods for inorganic anions, cations and some organic anions (plus fluoride) are reported elsewhere (Udisti

Table 1. IC parameters for determination of inorganic anions, cations and some organic anions

Separation column	Dionex AS11 + AG11	Dionex AS12A + AG12A	Dionex CS12A + CG12A
Eluent	$Na_2B_4O_7$ 1 mM	Na_2CO_3 2.7 mM + $NaHCO_3$ 0.3 mM	H_2SO_4 20 mN
Eluent flow	2 mL min^{-1}	1.5 mL min^{-1}	1 mL min^{-1}
Loop	1 mL	0.5 mL	0.5 mL
Detection limit (μg L^{-1})	Fluoride: 0.02	Chloride: 0.14	Sodium: 0.14
	Acetate: 0.09	Bromide: 0.10	Ammonium: 0.13
	Propionate: 0.15	Nitrate: 0.20	Potassium: 0.20
	Formate: 0.09	Phosphate: 0.40	Magnesium: 0.04
	MSA: 0.13	Sulphate: 0.19	Calcium: 0.13
	Pyruvate: 0.50		

Table 2. Concentration data for the ten subsamples around the volcanic layer (No. 7) for the Styx Glacier ice core

Sample No.	Depth	Na^+	Cl^-	$totSO_4^{2-}$	$nssSO_4^{2-}$	F^-	Acet.	Prop.	Form.	MSA	Pyruv.	NH_4^+	K^+	Mg^{2+}	Ca^{2+}	Br^-	NO_3^-	HPO_4^{2-}
	m	$\mu g\,L^{-1}$	$\mu g\,L^{-1}$	$\mu g\,L^{-1}$	$\mu g\,L^{-1}$	$\mu g\,L^{-1}$	$\mu g\,L^{-1}$	$\mu g\,L^{-1}$	$\mu g\,L^{-1}$	$\mu g\,L^{-1}$	$\mu g\,L^{-1}$	$\mu g\,L^{-1}$	$\mu g\,L^{-1}$	$\mu g\,L^{-1}$	$\mu g\,L^{-1}$	$\mu g\,L^{-1}$	$\mu g\,L^{-1}$	$\mu g\,L^{-1}$
1	93.23	70	128	67	50	1.5	16.3	0.7	24.3	6.3	1.8	25.4	23.0	8.5	53.6	0.32	75.1	4.1
2	93.26	102	183	140	114	7.7	5.9	0.4	9.5	7.4	d.l.	10.3	11.7	11.4	38.8	d.l.	55.3	2.4
3	93.29	71	242	81	63	4.4	5.4	0.2	6.7	4.6	d.l.	9.9	12.5	9.7	30.0	0.12	27.1	1.3
4	93.32	281	591	214	143	107.0	8.1	0.4	9.1	9.4	d.l.	12.1	34.1	14.8	65.7	d.l.	22.0	2.2
5	93.35	227	468	230	173	125.4	8.5	0.2	8.6	2.6	d.l.	14.9	53.2	16.4	42.3	0.12	13.3	1.5
6	93.38	1321	1789	344	10	397.1	14.5	0.5	38.7	14.6	d.l.	15.5	105.2	24.7	81.3	0.62	37.7	1.2
7	93.41	14527	5214	22310	18635	1296.8	154.6	4.8	628.2	287.5	1.9	74.7	346.8	88.3	1717.8	3.96	284.1	36.3
8	93.44	840	1007	251	39	16.8	20.1	0.6	114.3	3.6	0.6	23.9	31.2	8.7	56.6	2.18	186.6	4.5
9	93.47	115	148	95	66	2.1	10.9	d.l.	14.9	d.l.	d.l.	16.0	19.6	11.8	43.4	d.l.	66.2	3.0
10	93.50	108	233	83	56	1.5	4.4	d.l.	10.0	3.1	0.6	11.5	26.0	13.7	57.4	0.24	38.6	3.9

and others, 1991, 1994, 1998a, b). Table 1 summarises the techniques used for the analyzed compounds and the detection limits.

Figure 3 shows examples of the IC separations and identification of inorganic anions (Fig. 3a–b), and organic (plus fluoride) anions (Fig. 3c–d) for the more concentrated subsamples (dark layer 93.41 m depth).

DATA DISCUSSION

The concentration values for the determined substances are reported in Table 2. A series of numbers (the youngest, the dark-layer and the oldest subsamples are labelled 1, 7 and 10, respectively) identifies the ten subsamples. Also in Table 2 the depth of each subsample is reported. Figure 4 shows the concentration profiles of total sulphate ($totSO_4^{2-}$), $nssSO_4^{2-}$ and fluoride. The $nssSO_4^{2-}$ was calculated from the sodium content, used as a sea-spray marker, by

$$nssSO_4^{2-} = totSO_4^{2-} - swSO_4^{2-} = totSO_4^{2-} - 0.253\ Na^+,$$

where $swSO_4^{2-}$ means sea-water sulphate and 0.253 is the SO_4^{2-}/Na^+ ratio (w/w) in sea water.

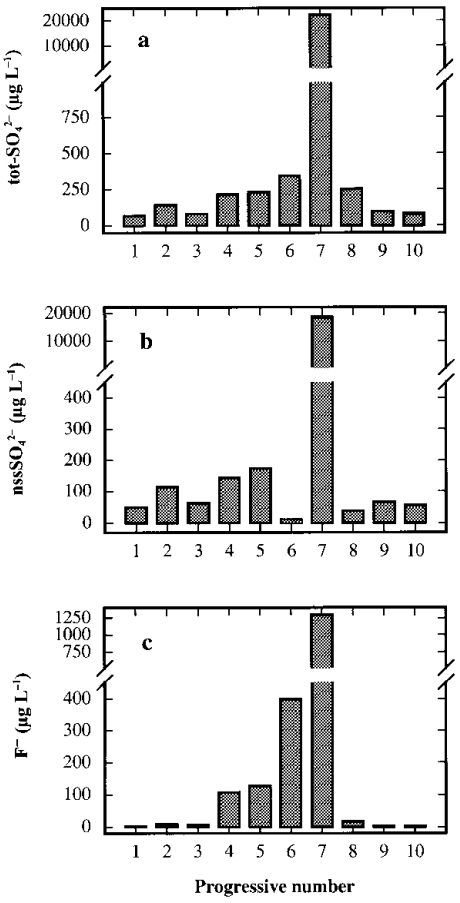

Fig. 4. Concentration/depth profiles of total sulphate (a), non-sea-salt sulphate (b) and fluoride (c) in the ten subsamples around the volcanic layer from 93.23 (sample 1) to 93.50 (sample 10) m depth.

Very high concentration peaks of sulphate and fluoride for the dark-layer sample (No. 7) show how these substances can be useful for the identification of volcanic events thanks to the massive emission of HF and SO_2 (successively oxidised to H_2SO_4). Fluoride and sulphate peaks, together with high values of acidity and conductivity, were detected in snow and ice layers recording volcanic eruptions from Greenland and Antarctica (Delmas and others, 1985, 1992; De Angelis and Legrand, 1994; Zielinski and others, 1997; Zreda-Gostynska and others, 1997; Aristarain and Delmas, 1998). The concentrations of $totSO_4^{2-}$ and $nssSO_4^{2-}$ (Fig. 4a and b) are very similar, so practically all the sulphate content can be ascribed to H_2SO_4. In sample 7, the concentration values for $nssSO_4^{2-}$ and F^- are 370 and 860 times higher, respectively, than in the ice-core-section extremities (samples 1 and 10). The $nssSO_4^{2-}$ concentration in sample 7 is about 220 times higher than the mean value (86.5 $\mu g\,L^{-1}$) measured in the same station by a 2.5 m snow pit (covering the period 1988–93) dug during the 1993–94 Italian Antarctic campaign (Table 3). Referring to the same dataset, the fluoride levels in the dark layer are about 1200 times higher than the mean 1988–93 value (0.99 $\mu g\,L^{-1}$). Detailed examination of the concentration profiles of fluoride (Fig. 4c), the marker showing the largest increase and the least influence by other source contributions, shows a typical atmospheric scavenging trend: the volcanic event starts with sample 8, where a concentration one order of magnitude higher than the mean was measured (16.8 $\mu g\,L^{-1}$), and reaches a maximum in sample 7. In successive samples, the F^- concentration quickly decreases, with a hyperbolic trend up to sample 1 in which it reaches the same concentration as sample 10.

The $nssSO_4^{2-}$ behaviour is similar, with the same low concentration in samples 1 and 10, and a maximum in sample 7, but the decrease is not constant, showing values 2–3 times higher than the background (samples 1 and 10), alternating

Table 3. Statistical concentration values for snow-pit samples (1988–93) collected in the Italian Antarctic campaign 1993–94

	Na^+	Cl^-	$totSO_4^{2-}$	$nssSO_4^{2-}$	F^-	*Acet.*	*Prop.*	*Form.*	*MSA*	*Pyruv.*	NH_4^+	K^+	Mg^{2+}	Ca^{2+}	Br^-	NO_3^-	HPO_4^{2-}
	$\mu g\,L^{-1}$	$\mu g\,L^{-1}$	$\mu g\,L^{-1}$	$\mu g\,L^{-1}$	$\mu g\,L^{-1}$	$\mu g\,L^{-1}$	$\mu g\,L^{-1}$	$\mu g\,L^{-1}$	$\mu g\,L^{-1}$	$\mu g\,L^{-1}$	$\mu g\,L^{-1}$	$\mu g\,L^{-1}$	$\mu g\,L^{-1}$	$\mu g\,L^{-1}$	$\mu g\,L^{-1}$	$\mu g\,L^{-1}$	$\mu g\,L^{-1}$
Number of data	76	76	76	76	76	76	76	76	76	76	76	76	76	76	33	76	28
Min.	8.7	20.7	17.3	5.9	0.14	6.48	0.36	2.51	3.8	0.71	0.79	2.68	2.0	10.4	0.20	4.8	1.35
Max.	1520.0	2886	435.4	420.1	4.04	39.37	7.20	25.41	129.6	10.05	12.24	74.12	200.7	145.9	16.44	246.7	10.95
Mean	111.2	215.0	105.5	77.7	0.99	15.73	2.13	10.03	21.0	2.78	2.65	10.72	16.9	36.9	2.07	48.8	4.78
Std dev.	192.1	357.5	81.2	70.0	0.73	6.39	1.22	5.64	22.8	2.32	1.67	10.32	24.9	26.6	3.72	33.1	2.58

with low values (samples 6 and 3). Further contributions, naturally variable, of sulphate and above all, of Na^+ (sample 6) used for the $nssSO_4^{2-}$ calculation can mask the observation of the scavenging processes of volcanic $nssSO_4^{2-}$.

The dominance of the scavenging effect on possible simple processes of diffusion of the various components between contiguous snow layers seems to be proved by the asymmetry of the concentration profiles. Table 2 shows higher values for sample 6 (layer younger than sample 7) than for sample 8 (layer older than sample 7) for all the components forming soluble salts, such as Na^+, Cl^-, $totSO_4^{2-}$, MSA, K^+, Mg^{2+} and Ca^{2+}. Diffusion processes should have caused a similar increase in the contiguous layers or, better, a higher increase in the oldest layer by the longer contact time. Instead, some compounds prevalently associated with gas phase (carboxylic acids, NO_3^-, NH_4^+ and Br^-) show higher concentrations in sample 8 than in sample 6. This evidence could support the hypothesis of a gas emission just before the massive volcanic event.

A sudden increase of concentration in sample 7 is shown by all the analyzed components, although the increase is lower than that shown by fluoride and sulphate. Figure 5 shows the concentration profiles for Ca^{2+} (Fig. 5a), MSA (Fig. 5b) and phosphate (Fig. 5c). These compounds show concentration peaks in sample 7 about 30, 70 and 10 times higher, respectively, than the background values, but the concentration levels fall immediately to the background values in samples 6 and 8. This pattern is consistent with the hypothesis that the volcanic event was very time-limited and/or the source was near enough to collect the soil particles emitted in the atmosphere. In particular, Ca^{2+} can be used as a crustal indicator (the Ca^{2+}/Na^+ ratio in sample 7 is twice as high as in samples 6 and 8) and MSA is solely produced by biogenic marine activity, so it cannot be directly correlated to the volcanic input (ash). Phosphate, too, can be attributed to biogenic activity, but this source is not unique. Therefore, the high concentrations of calcium, MSA and phosphate in sample 7 seem to be ascribable, not to volcanic ash, but to the contribution of soil particles. In fact, the only explanation for high concentrations of MSA is gradual accumulation on the top and the slopes of the volcano by deposition and successive melting of snow precipitations. At the moment of the eruption, a quantity of the surface soil could be emitted into the atmosphere in addition to the normal ash emission. The short half-lives of these rather large soil particles caused their fast deposition, by wet or dry removal processes, so that the atmospheric scavenging was already complete at the time of the successive snow depositions (sample 6).

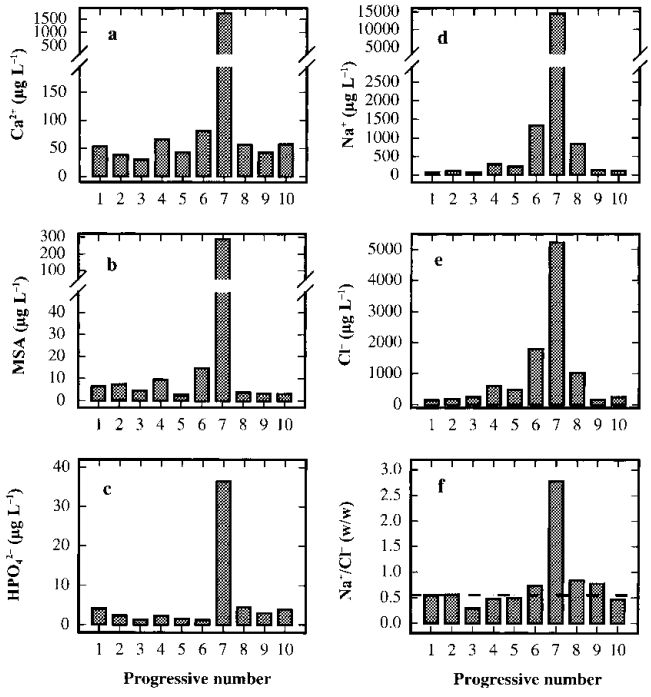

Fig. 5. Concentration/depth profiles of calcium (a), MSA (b), phosphate (c), sodium (d) and chloride (e), and trend of the Na^+/Cl^- w/w ratio (f), in the ten subsamples around the volcanic layer from 93.23 (sample 1) to 93.50 (sample 10) m depth.

Furthermore, the MSA profile unarguably shows the absence of diffusion effects. Actually, for this compound, the only known source is biogenic, and its concentration profile cannot be misinterpreted by any secondary source or particular transport phenomena. The MSA concentration in the layers contiguous to the dark layer falls immediately to background levels ($<10\,\mu g\,L^{-1}$), values that are similar to the 1988–93 mean (21.0 $\mu g\,L^{-1}$; Table 3). Some authors report a seasonal dephasing between MSA and $nssSO_4^{2-}$ (with summer $nssSO_4^{2-}$ and winter MSA peaks) due to possible diffusion of MSA in recent and old snow layers in stations located in the Antarctic Peninsula (Mulvaney and others, 1992) and in the Filchner–Ronne Ice Shelf (Wagenbach and others, 1994). In our experience, this anomaly is absent from snow pits and shallow firn cores collected in northern Victoria Land (Piccardi and others, 1996b; Udisti, 1996; Udisti and others, 1998b; Stenni and others, unpublished). The Styx Glacier medium-depth ice core confirms our previous observation that in a 500 year period no significant diffusion is shown between two contiguous snow layers, about 10 mm apart, with a concentration ratio of 80:1 (sample 7/sample 8).

Na^+ and Cl^- (Fig. 5d and e) show a lower increase in sample 7 compared with the two samples around the dark layer. The Na^+ content in sample 7 is about one order of magnitude higher than in samples 6 and 8, but the Cl^- content is only five times higher. However, the Na^+ peak is about 100 times higher than the 1988–93 mean value at the same station (Table 3), so the contribution of the sea salt accumulated on the soil particles seems also to be dominant in this case. The fundamental difference between sample 7 and contiguous samples is shown in Figure 5f, which gives the Na^+/Cl^- ratios for the ten samples. In all other samples, the Na^+/Cl^- ratio is very similar to the sea-water composition ($Na^+/Cl^- = 0.55$ w/w; dashed line in Fig. 5f), so the sea-spray source seems apparent. The relatively high concentrations in samples 6 and 8, therefore, may be due to the normal variability in the sea-salt content in snow. Data from snow pits and shallow firn cores show that values higher than 1 mg L^{-1} for Na^+ and Cl^- are not unusual for this station, corresponding to snow precipitation with sea winds (Piccardi and others, 1994a, b, 1996a). For sample 7, however, the Cl^-/Na^+ ratio is dramatically different and shifted to an Na^+ preponderance ($Na^+/Cl^- = 2.8$ w/w). This pattern can be explained by the fact that following the volcanic event, the atmospheric aerosol was enriched by very high concentrations of H_2SO_4 and other acids. In fact, acidity measurements are a simple method of identifying volcanic layers in snow and ice (Hammer and others, 1980). The NaCl included in the atmospheric aerosol and on the soil particles can react with H_2SO_4 to give Na_2SO_4 and gaseous HCl (Mayewski and others, 1993).

$$H_2SO_4 + 2NaCl \rightarrow Na_2SO_4 + 2HCl \uparrow .$$

The gas-phase HCl may not be deposited in the ice, while Na_2SO_4 is deposited by dry and/or wet (snow) deposition. Two observations can be made:

The Na^+/Cl^- ratio returns quickly to sea-water values. Going to sample 6 from sample 7, the ratio changes from 2.8 to 0.74, approaching the theoretical value of 0.55.

The variation of Na^+/Cl^- ratio could confirm the source closeness, too, as the supposed exchange mechanism between H_2SO_4 and NaCl involves two processes:

(1) near the source: the deposition of Na_2SO_4 and the sending away of gaseous HCl with an increase of the Na^+/Cl^- ratio;

(2) far from the source: the deposition of HCl with a decrease of the Na^+/Cl^- ratio.

Mg^{2+} and K^+ follow the same trend as Na^+, showing that sea spray is an important source, but with lower peaks in sample 7 (about 9 and 14 times the background values, respectively).

Figure 6 shows the concentration profiles for NH_4^+, NO_3^- and Br^-. These components, as already mentioned, have a peculiarity: the concentration peaks in sample 7 do not show high enrichments with respect to background values (about 5, 7 and 10 times, respectively), but like F^-, their concentration in sample 8 (just before the volcanic event) is significantly higher than the background. Moreover, for NO_3^- and Br^- the concentration in sample 8 is higher than in sample 6 (just after the dark layer) and comparable with sample 7. This is also true, but less evident, for NH_4^+. A significant contribution to snow composition by dry deposition (probably snow-surface adsorption) and/or

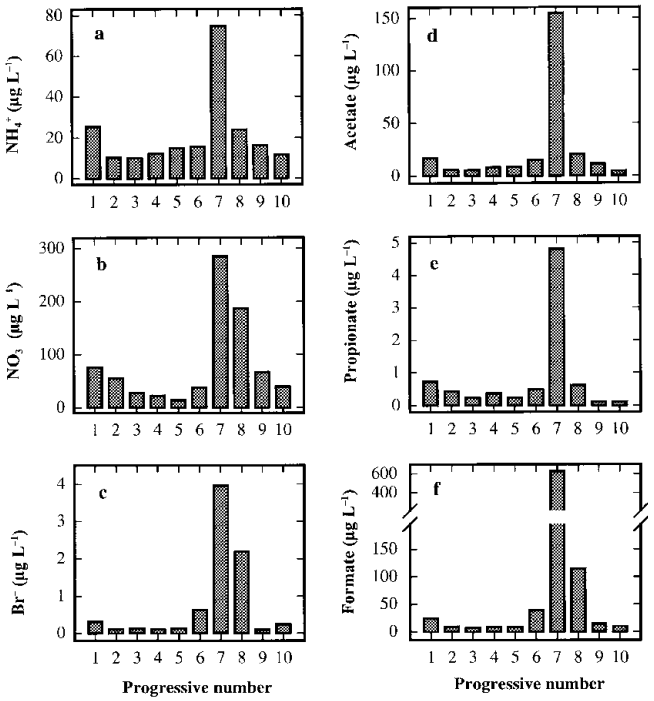

Fig. 6. Concentration/depth profiles of ammonium (a), nitrate (b), bromide (c), acetate (d), propionate (e) and formate (f) in the ten subsamples around the volcanic layer from 93.23 (sample 1) to 93.50 (sample 10) m depth.

wet deposition of HNO_3 and HBr (as well as F^-), directly emitted or built up as secondary volcanic products, must be taken into account.

Finally, some short-chain carboxylic acids show high concentrations in sample 7 (Fig. 6). Peak concentrations 10–20 times higher than the background values were measured for acetic, propionic and formic acids. In particular, formate has the highest concentration, reaching a value about 60 times higher than the mean 1988–93 value (10.03 μg L^{-1}; Table 3). The concentration of the carboxylic acids, too, are higher in sample 6 than in sample 8, confirming the similar pattern of atmospheric gas-phase distribution compounds.

Many sources were postulated for carboxylic acids in polar atmosphere, such as direct input from biologic activity and vegetation, secondary emission by oxidation of marine and continental biogenic hydrocarbons or biomass-burning, and from anthropogenic activity (Talbot and others, 1990; Legrand and De Angelis, 1996; Udisti and others, 1998a). Measurements of acetic, propionic and formic acids in polar snow are sporadic, and no correlation was reported between their increase and the volcanic activity. Legrand and De Angelis (1996) report an inverse correlation between carboxylic-acid concentrations in the snow and high acidic content in the atmosphere such as happens during a volcanic eruption. Even so, in Antarctica their production is mainly related to carbon-cycle oxidation processes, so they could also be built up by oxidation of hydrocarbons emitted by volcanic activity. For example, Brimblecombe (1996) reports a CH_4 global flux of 0.34 Tg a^{-1} from volcanic input. When the carboxylic-acid measurements are available for Antarctic ice cores, where anthropogenic, biomass-burning and vegetation emissions are very small, the correlation with volcanic activity will be verified.

What is the source?

A comparison with the explosive volcanic records at South

Pole in the last 1000 years (Delmas and others, 1992) did not give unambiguous information to identify the source. No eruptions were reported for the period around AD 1500. The Ruiz and Huaynaputina eruptions (dating of the signal: AD 1596 and 1601, respectively) have a large time difference from the Styx event dating (about 50 years). Besides, their sulphate signals in the ice are not as large as that found in the Styx Glacier volcanic layer. A high sulphate peak characterises the closer eruption around AD 1450. Delmas and others (1992) suggest that Deception Island or Sandwich Island could be the source. Zielinski (1995) attributes the 1450 volcanic signal to the Kuwae eruption (GISP2 Greenland ice-core analysis). A better comparison will be carried out once a more reliable dating of Styx Glacier ice core is available by chemical and isotopic $\delta^{18}O$ profiles (now in progress), and using time-reference horizons.

The thickness of the dark layer and, above all, the fast decrease of all the marker concentrations within a very short distance of the zone with the highest values suggest that this is a local volcanic event. Besides, a contribution of dry deposition of particulate material containing relatively large soil particles is evident, in addition to the ash deposition. This is shown by high concentrations of typical crustal substances such as Ca^{2+}, Mg^{2+} and K^{+} and of other compounds that cannot be related to volcanic ash but only to soil-accumulation processes by snow-melting, such as MSA and phosphate. These relatively large soil particles can reach the deposition site by two principal processes: fast dry deposition if the source is near, or injection into the high troposphere (or into the stratosphere) in the case of explosive volcanic events for very distant sources. In the second case, however, a longer half-life in the atmosphere is predictable, with the removal processes (by dry and wet depositions) continuing for a long time, leading to the markers being recorded in a thicker ice-core layer.

The Styx Glacier station is located about 40 km from the Mount Melbourne volcano, the eruptive activity of which is described by Worner and others (1989), Armienti and others (1991), Horning and others (1991) and Lanzafame and Villari (1991). Structural and chemical analysis of the ice-core particulate compared to Mount Melbourne eruption deposits will clarify whether this is the source.

A more probable source is Mount Erebus, a still fully active volcano about 300 km from Styx Glacier. Zreda-Gostynska and others (1997) report high concentrations of HF in gas and aerosol measurements of Mount Erebus emissions, and support F^{-} concentration in snow being a tracer for Erebus volcanic activity. Zreda-Gostynska and others (1997) estimate an HF emission rate of 2.3–9.2 Gg a^{-1} in the period December 1986–January 1991, with an air concentration of 2.5–5 ng m^{-3} and a residence time of 10–21 days. Mount Erebus also emits H_2SO_4 (25.9 $\pm$ 7.3 Gg a^{-1} as SO_2 in January 1991), but this contribution is less distinctive and comprises only a small percentage (about 3%) of the total sulphur budget in the Antarctic atmosphere.

Aristarain and Delmas (1998) report a well-marked volcanic ash layer in a 145.9 m ice core from James Ross Island and attribute it to Deception Island volcano (around AD 1641). A comparison between the chemical markers reported by Aristarain and Delmas and our data seems unsatisfactory. The time shift is too large, even considering that our dating is not definitive. Similar Cl^{-} depletion, with respect to the sea-water Na^{+}/Cl^{-} ratio, is reported, but no increase of nitrate is shown in the Deception Island eruption, and the sulphate increase is much smaller (only about 4.5 times higher than the background level), even if the ice-core station (James Ross Island) is rather close to (about 200 km from) the source. For the Styx Glacier ice core, located about 4500 km from Deception Island, sulphate concentration in the dark layer is 370 times higher than the background level. Aristarain and Delmas report no fluoride data. They also report the chronological scale of the Deception Island eruptions in the last millennium, indicating a volcanic event dated around AD 1550 identified by marine and lake sediment (Fildes Peninsula–Bransfield Strait Area). Unfortunately, the James Ross ice core is too short to characterise such an eruption in the snow.

Volcanoes located outside Antarctica or even in the Northern Hemisphere seem to be less probable sources. Long-range transport processes are highly dependent on the event intensity and meteorological conditions, such as seasonality and strength and direction of the winds. Measurements performed on various transport tracers (Wagenbach, 1996) showed that the characteristic time for the inter-hemispheric exchange is around 1 year. This is more than an order of magnitude greater than the typical tropospheric aerosol residence time. Therefore, only cataclysmic events of global concern can be recorded in snow and ice cores. In the Styx volcanic layer, a cataclysmic explosive eruption can be excluded, since it would be memorized in all Antarctic ice cores due to the very high-concentrate deposits, and only a regional input seems probable. Therefore, we conclude that the source is located in the Southern Hemisphere, probably on the Antarctic continent.

CONCLUSIONS

A roughly 500 year-old volcanic event was identified and characterised by chemical analysis of a 110 m ice core drilled at Styx Glacier plateau.

The event was characterised by a gas emission (HF, SO_2 and probably HBr, HNO_3 and NH_3) followed by a volcanic eruption with emission of ash and probably soil particulate into the atmosphere. Gas-phase and particulate atmospheric scavenging occurred by dry and wet removal processes in a very short time (about 10 mm ice layer in a station with a mean snow accumulation rate of about 160 kg m^{-2} a^{-1}; Piccardi and others, 1994a; Udisti, 1996; Stenni and others, unpublished). The most obvious markers were HF and H_2SO_4 for gas-phase emission and Ca^{2+} and MSA (indirect indicators) for soil-particulate scavenging. Significant concentrations of nitrate, ammonium and bromide are present in and directly beneath the dark layer, indicating a possible early emission as gas-phase compounds. The possibility that high concentrations of some carboxylic acids (acetic, propionic and formic) can constitute a volcanic marker needs to be confirmed.

The acidic emission (primarily H_2SO_4) probably caused a sharp increase of Na^{+}/Cl^{-} ratio with respect to the sea-water composition by HCl removal.

No significant diffusion between adjacent snow layers (resolution 30 mm) was shown by the concentration/depth profiles.

A source attribution of the Styx Glacier volcanic event is not yet possible. The most likely candidate is Mount Erebus, in view of its massive fluoride emission and its proximity. The chemical and structural analysis of the particulate, now in progress, will clarify the problem.

ACKNOWLEDGEMENTS

This research was carried out in the framework of a project on glaciology and palaeoclimatology of the Programma Nazionale di Ricerche in Antartide. It was financially supported by Ente per le Nuove Tecnologie, l'Energia e l'Ambiente through a cooperative agreement with Università di Milano.

REFERENCES

Aristarain, A. J. and R. Delmas. 1998. Ice record of a large eruption of Deception Island volcano (Antarctica) in the XVIIth century. *J. Volcanol. Geotherm. Res.*, **80**(1–2), 17–25.

Armienti, P. *and 6 others*. 1991. New petrologic and geochemical data on Mt. Melbourne volcanic field, northern Victoria Land, Antarctica (II Italian Antarctic Expedition). *Mem. Soc. Geol. Ital.* 46, 397–424.

Brimblecombe, P. 1996. *Air composition and chemistry. Second edition.* Cambridge, Cambridge University Press.

Clausen, H. B. and C. U. Hammer. 1988. The Laki and Tambora eruptions as revealed in Greenland ice cores from 11 locations. *Ann. Glaciol.*, **10**, 16–22.

De Angelis, M. and M. Legrand. 1994. Origins and variations of fluoride in Greenland precipitation. *J. Geophys. Res.*, **99**(D1), 1157–1172.

Delmas, R. J., M. Legrand, A. J. Aristarain and F. Zanolini. 1985. Volcanic deposits in Antarctic snow and ice. *J. Geophys. Res.*, **90**(D7), 12,901–12,920.

Delmas, R. J., S. Kirchner, J. M. Palais and J. -R. Petit. 1992. 1000 years of explosive volcanism recorded at the South Pole. *Tellus*, **44B**(4), 335–350.

Goodwin, I. D. 1990. Snow accumulation and surface topography in the katabatic zone of eastern Wilkes Land, Antarctica. *Antarct. Sci.*, **2**(3), 235–242.

Hammer, C. U. 1989. Dating by physical and chemical seasonal variations and reference horizons. *In* Oeschger, H. and C. C. Langway, Jr, *eds. The environmental record in glaciers and ice sheets*. Chichester, etc., John Wiley and Sons, 99–121.

Hammer, C. U., H. B. Clausen and W. Dansgaard. 1980. Greenland ice sheet evidence of post-glacial volcanism and its climatic impact. *Nature*, **288**(5788), 230–235.

Handler, P. 1989. The effect of volcanic aerosols on global climate. *J. Volcanol. Geotherm. Res.*, **37**, 233–249.

Herron, M. M. and C. C. Langway, Jr. 1980. Firn densification: an empirical model. *J. Glaciol.*, **25**(93), 373–385.

Horning, I., G. Worner and J. Zipfel. 1991. Lower crustal and mantle xenoliths from the Mt. Melbourne volcanic field, northern Victoria Land, Antarctica. *Mem. Soc. Geol. Ital.* 46, 337–352.

Langway, C. C., Jr, H. B. Clausen and C. U. Hammer. 1988. An inter-hemispheric volcanic time-marker in ice cores from Greenland and Antarctica. *Ann. Glaciol.*, **10**, 102–108.

Lanzafame, G. and L. Villari. 1991. Structural evolution and volcanism in northern Victoria Land (Antarctica): data from Mt. Melbourne–Mt. Overlord–Malta Plateau region. *Mem. Soc. Geol. Ital.* 46, 371–381.

Legrand, M. and M. de Angelis. 1996. Light carboxylic acids in Greenland ice: a record of past forest fires and vegetation emissions from the boreal zone. *J. Geophys. Res.*, **101**(D2), 4129–4145.

Legrand, M. R. and R. J. Delmas. 1987. A 220-year continuous record of volcanic H_2SO_4 in the Antarctic ice sheet. *Nature*, **327**(6124), 671–676.

Ling, C.H. 1985. A note on the density distribution of dry snow. *J. Glaciol.*, **31**(108), 194–195.

Mayewski, P. A. *and 8 others*. 1993. Greenland ice core "signal" characteristics: an expanded view of climate change. *J. Geophys. Res.*, **98**(D7), 12,839–12,847.

Mulvaney, R., E. C. Pasteur, D. A. Peel, E. S. Saltzman and P. -Y. Whung. 1992. The ratio of MSA to non-sea-salt sulphate in Antarctic Peninsula ice cores. *Tellus*, **44B**(4), 295–303.

Palais, J. M., S. Kirchner and R. J. Delmas. 1990. Identification of some global volcanic horizons by major element analysis of fine ash in Antarctic ice. *Ann. Glaciol.*, **14**, 216–220.

Pettré, P., J. F. Pinglot, M. Pourchet and L. Reynaud. 1986. Accumulation distribution in Terre Adélie, Antarctica: effect of meteorological parameters. *J. Glaciol.*, **32**(112), 486–500.

Piccardi, G., R. Udisiti and F. Casella. 1994a. Seasonal trends and chemical compositon of snow at Terra Nova Bay (Antarctica). *Int. J. Environ. Anal. Chem.*, **55**, 219–234.

Piccardi, G., E. Barbolani, S. Bellandi, F. Casella and R. Udisti. 1994b. Spatial and temporal trends of snow chemical composition of northern Victoria Land (Antarctica). *Terra Antartica 1, 134–137.*

Piccardi, G., S. Becagli, R. Traversi and R. Udisti. 1996a. Fractionating phenomena, altitude induced, on snow composition in northern Victoria Land (Antarctica). *In* Colacino, M., G. Giovannelli and L. Stefanutti, *eds. Conference on Italian Research on Antarctic Atmosphere, 6–8 November 1995, Florence, Italy. Proceedings. Vol. 51.* Bologna, Società Italiana di Fisica, 229–245.

Piccardi, G., F. Casella and R. Udisti. 1996b. Non-sea-salt contribution of some chemical species to the snow composition at Terra Nova Bay (Antarctica). *Int. J. Environ. Anal. Chem.*, **63**, 207–223.

Rampino, M. R. and S. Self. 1992. Volcanic winter and accelerated glaciation following the Toba super-eruption. *Nature*, **359**(6390), 50–52.

Talbot, R.W., M. O. Andreae, H. Berresheim, D. J. Jacob and K. M. Beecher. 1990. Sources and sinks of formic, acetic and pyruvic acids over central Amazonia. 2. Wet season. *J. Geophys. Res.*, **95**(D10), 16,799–16,811.

Udisti, R. 1996. Multiparametric approach for chemical dating of snow layers from Antarctica. *Int. J. Environ. Anal. Chem.*, **63**, 225–244.

Udisti, R., E. Barbolani and G. Piccardi. 1991. Determination of some organic and inorganic substances present at ppb level in Antarctic snow and ice by ion chromatography. *Ann. Chim.*, **81**(7–8), 325–341.

Udisti, R., S. Bellandi and G. Piccardi. 1994. Analysis of snow from Antarctica: a critical approach to ion-chromatographic methods. *Fresenius' J. Anal. Chem.*, **349**(4), 289–293.

Udisti, R., S. Becagli, R. Traversi, S. Vermigli and G. Piccardi. 1998a. Preliminary evidence of a biomass-burning event from a 60 year-old firn core from Antarctica by ion chromatographic determination of carboxylic acids. *Ann. Glaciol.*, **27**, 391–397.

Udisti, R., R. Traversi, S. Becagli and G. Piccardi. 1998b. Spatial distribution and seasonal pattern of biogenic sulphur compounds in snow from northern Victoria Land, Antarctica. *Ann. Glaciol.*, **27**, 535–542.

Wagenbach, D. 1996. Coastal Antarctica: atmospheric chemical composition and atmospheric transport. *In* Wolff, E. W. and R. C. Bales, *eds. Chemical exchange between the atmosphere and polar snow.* Berlin, etc., Springer-Verlag, 173–199. (NATO ASI Series I: Global Environmental Change 43.)

Wagenbach, D. *and 6 others*. 1994. Reconnaissance of chemical and isotopic firn properties on top of Berkner Island, Antarctica. *Ann. Glaciol.*, **20**, 307–312.

Worner, G., H. Niephaus, J. Hertogen and L. Viereck. 1989. The Mt. Melbourne volcanic field (Victoria Land–Antarctica). II. Geochemistry and magma genesis. *Geol. Jahrb., Ser. E*, **38**, 395–433.

Zielinski, G. A. 1995. Stratospheric loading and optical depth estimates of explosive volcanism over the last 2100 years derived from the Greenland Ice Sheet Project 2 ice core. *J. Geophys. Res.*, **100**(D10), 20,937–20,955.

Zielinski, G. A., J. E. Dibb, Q. Yang, P. A. Mayewski, S. Whitlow and M. S. Twickler. 1997. Assessment of the record of the 1982 El Chichon eruption as preserved in Greenland snow. *J. Geophys. Res.*, **102**(D25), 30,031–30,045.

Zreda-Gostynska, G., P. R. Kyle, D. Finnegan and K. M. Prestbo. 1997. Volcanic gas emissions from Mount Erebus and their impact on the Antarctic environment. *J. Geophys. Res.*, **102**(B7), 15,039–15,055.